USING CLOUD CLASSIFICATION TO MODEL SOLAR VARIABILITY

Matthew J. Reno
Sandia National Laboratories
Georgia Institute of Technology
777 Atlantic Drive NW
Atlanta, GA 30332-0250, USA
matthew.reno@gatech.edu

Joshua S. Stein
Sandia National Laboratories
P.O. Box 5800
Albuquerque, NM 87185, USA
jsstein@sandia.gov

ABSTRACT

Imagery from GOES satellites is analyzed to determine how solar variability is related to the NOAA classification of cloud type. Without using a model to convert satellite imagery to average insolation on the ground, this paper investigates using cloud categories to directly model the expected statistical variability of ground irradiance. Hourly cloud classified satellite images are compared to multiple years of ground measured irradiance at two locations to determine if measured irradiance, ramp rates, and variability index are correlated with cloud category. Novel results are presented for ramp rates grouped by the cloud category during the time period. This correlation between satellite cloud classification and solar variability could be used to model the solar variability for a given location and time and could be used to determine the variability of a location based on the prevalence of each cloud category.

1. INTRODUCTION

With increasing amounts of solar energy on the electric grid, understanding the solar variability for different regions and times of year is important, especially under high penetrations of PV on the distribution system where variability can create voltage flicker and increased degradation of voltage regulation equipment, leading to shorter lifetimes. PV interconnection impact studies are performed to analyze possible impacts to the grid, but these studies require a valid model of the PV plant output at a short timescale to model the impact of the output variability to the grid [1, 2].

Regular images from geostationary satellites can be used to detect and track weather patterns. This imagery is freely available everywhere in the United States and is commonly used to estimate the ground irradiance when local irradiance measurements are not available. The satellite images are taken every 15 minutes or hourly, so obtaining high time-resolution data or irradiance ramp rates can be difficult. This paper investigates using satellite imagery to model the expected statistical variability of ground irradiance without using a model to convert satellite imagery to average insolation on the ground. The objective is to investigate what characteristics of the performance of a solar power system can be distinguished by the type of cloud or weather pattern, as classified by NOAA. Instinctively, the type of cloud affects the expected cloud size and the amount of light blocked, so the variability at a given time should depend on the cloud type and weather pattern present at the site.

This correlation between satellite cloud classification and solar variability could have many applications for predicting variability or ramp rates at locations with PV plants. For example, if the cloud type is known, or forecasted, control algorithms for energy storage, spinning reserve, or optimal dispatch could be controlled based on the expected variability and ramp rates from solar power plants for that period. It could also be used to model the solar variability for a given location and time by synthetically creating time series irradiance data. The frequency of each cloud category could be used to distinguish the differences in variability for different locations and regions.

2. BACKGROUND

Classifying the types and properties of each cloud class is an interesting research problem that historically was done by trained human observers. With satellite images and data, clouds and weather patterns can be classified for large geographic areas. From the ground, sensors such as irradiance sensors can categorize cloud cover or cameras with image processing can detect and recognize types of clouds. Tapakis and Charalambides provide a detailed overview of all methods for detecting and classifying clouds using the full variety of sensors and cameras on the ground or in space [3].

While the goal of the research shown in this paper is to characterize ground irradiance from cloud type, several researchers have investigated the reverse process of classifying the type of cloud using ground sensor measurements. Duchon and O'Malley defined a cloud classification method using time series data from a pyranometer to categorize clouds into one of seven types with a 21 minute running mean and standard deviation of irradiance [4]. In [5], this method was found to be usable for classifying the clouds in Antarctica, and more detailed and accurate criteria were proposed. Another method proposed using time series global and diffuse irradiance data and five different statistical metrics to cluster the time series data into several classes and determine the number of oktas with cloud cover [6]. In South Dakota, a four band (440 to 936 nm) photometer measured shape was fit into one of nine cloud types using a decision tree [7]. Finally, a method was developed to classify clouds with combinations of attenuations in the beam transmittance and visual identification from sky images [8].

Image processing can provide autonomous classification of clouds from images taken from the ground at regular intervals. In [9], sky photographs were used to create cloud contours with fractals, synthesize cloud patterns, and create time series irradiance data. A whole sky imaging system was used in [10] and [11] to classify cloud types in the image based on color and texture.

The spatial cloud variability can be used to classify clouds into five different classes, where each cloud class relates to a irradiance variability class [12]. The irradiance variability class allows an irradiance time series to be synthetically created that statistically represents the expected measured irradiance on the ground.

3. GSIP (GOES SURFACE AND INSOLATION PRODUCTS) CLOUD DATA

Our research investigates the information that can be derived directly from the GOES Surface and Insolation Products (GSIP) cloud type. GSIP is a high spatial resolution (1/8 x 1/8 degrees) solar radiation product created by NOAA from processed GOES satellite data [13]. For the continental United States, this results in approximately 10×10 km pixels estimated from the GOES-East and GOES-West imager radiance measurements every hour. The products contain upwelling and downwelling shortwave and visible radiative fluxes, cloud fraction, cloud phase, visible cloud optical depth, outgoing longwave radiation, composite clear and cloudy reflectance, and total column amounts of water vapor and ozone.

NOAA processes GSIP data using all five imaging channels on GOES, NCEP GFS forecast model data, and IMS daily snow data. The algorithm detects clouds and determines the cloud fraction, dominant cloud type, and radiative fluxes. The GSIP parameter under investigation is the classified cloud type. This paper compares the NOAA declared cloud type to the irradiance pattern on the ground to determine if there is a connection between cloud type and variability.

4. CLEARNESS AND CLEAR SKY INDICIES

As solar irradiance on the ground varies with time and location, all analysis of the impact of cloud cover on the ground is performed in this paper using the "clear sky" index. This allows the analysis to identify the percent of solar radiation blocked by type of cloud, removing the time and locational dependence. The clearness index can be directly calculated from the extraterrestrial radiation, but to remove the locational dependence, clear sky index is calculated using a clear sky model. While none of these clear sky models are perfect, they provide a much more accurate representation of the expected shape for clear sky irradiance on the ground [14, 15]. The clear sky model used here is the Ineichen model [16]. The inputs to this model are solar zenith (z), air mass (AM), Linke Turbidity (TL), and elevation (*h*). Kasten and Young's formula is used to calculate the air mass [17]. Remund calculated and produced Linke turbidity maps for the world for each month using a combination of ground measurement and satellite data [18] that can be downloaded from either the HelioClim website [19] or Solar Radiation Data (SoDa) website [20].

5. VISUALLY COMPARING CLOUD CATEGORY TO MEASURED GROUND IRRADIANCE

The figures below show examples of how the solar variability is related to cloud type. In each figure, the satellite image with the color coding for cloud type is shown above the daily timeseries ground measurement. The ground irradiance sensor is in the center of the image marked with a small green square.
The cloud type numbers always refer to the NOAA cloud type classification, and the colors in the figures are consistent throughout the paper for cloud type. The cloud type legend and descriptions are shown in Fig. 1.

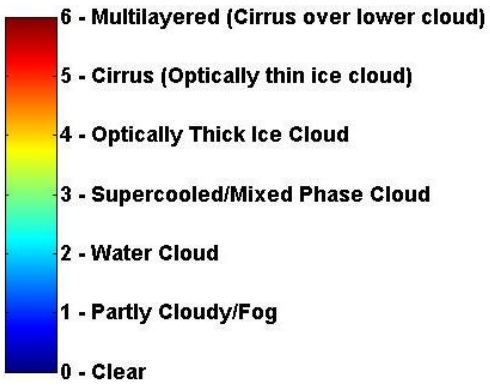

Fig. 1: Legend for GSIP cloud types.

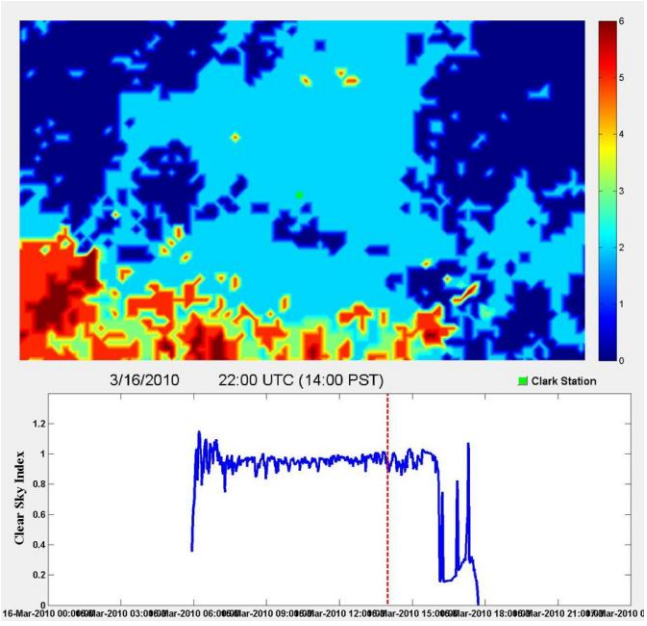

Fig. 2: Low variability with water clouds (Type 2).

In Fig. 2 the water clouds are shown to have low variability. In Fig. 3 the optically thick ice clouds have a significant impact on the average irradiance on the ground, but the variability is low with a fairly constant low clear sky index.

While variability is correlated with the cloud type overhead, other factors may also play an important role. For example in Fig. 4, the day has high temporal variability from the spatial variability of different types of clouds as they pass overhead. Very small clouds also may not show up on the satellite images.

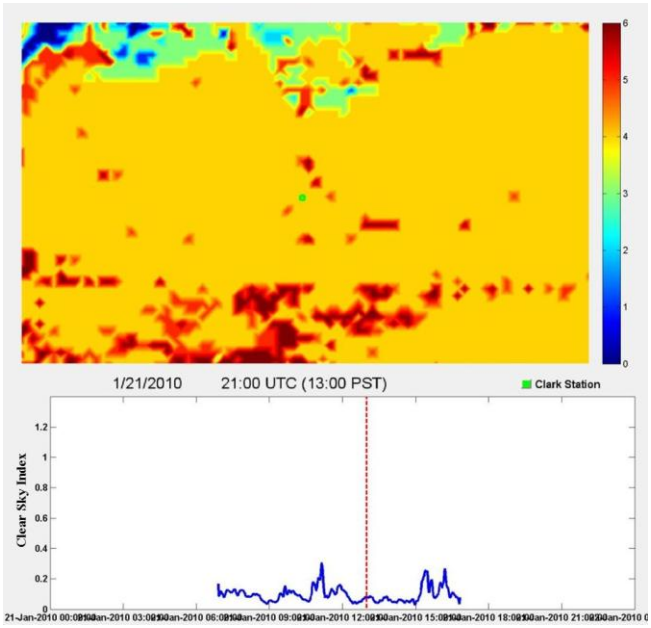

Fig. 3: Low irradiance and low variability with optically thick clouds (Type 4).

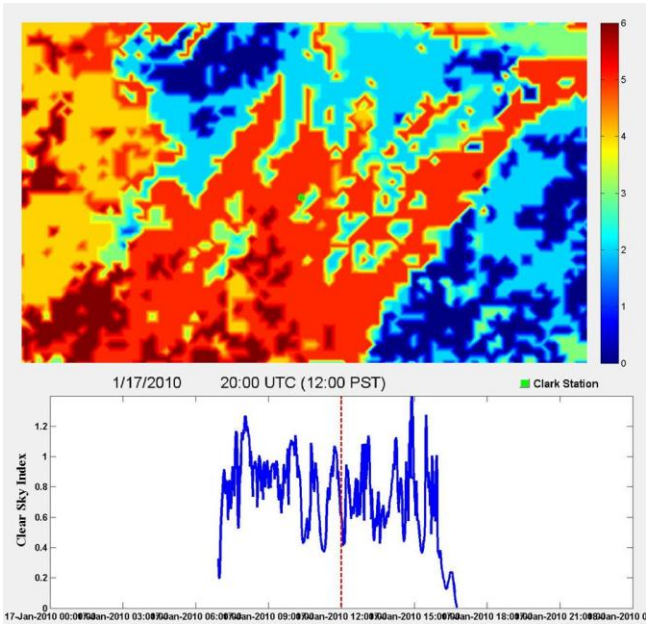

Fig. 4: High variability coming from spatial variability in different cloud types.

6. ANALYSIS DATA

Analysis is performed with GOES West northern hemisphere extended scan sector GSIP data. For GOES West, the GSIP images are on the hour each hour of the day. The 20,000 hourly images from April 2009 to July 2011 were downloaded [13], totaling ~350 GB of data. The satellite images are compared to global horizontal irradiance at two locations during the same time period. Both locations are part of the NREL MIDC database [21]. The irradiance measurements are logged at 1-minute resolution. UNLV is the University of Nevada, Las Vegas, and Anatolia is in Rancho Cordova, California.

For the analysis, the hourly satellite images are cropped to a 4x4 pixel window around the ground irradiance sensor site. This provides roughly a 40 km square around the irradiance measurement point. With only hourly images, the 40 km square is used to represent the irradiance time series information for the 30 minutes before and after the image is taken. The cropped satellite image is processed for the mean cloud type, largest number cloud type, smallest number cloud type, and the range of cloud types in the 16 pixels. These cloud statistics are analyzed and compared to the 60 minute clear sky index time series around the image snapshot.

The frequency of specific cloud types will be different between geographical areas. The distribution of average cloud types for all daylight hours for Anatolia and UNLV is shown in Fig. 5.

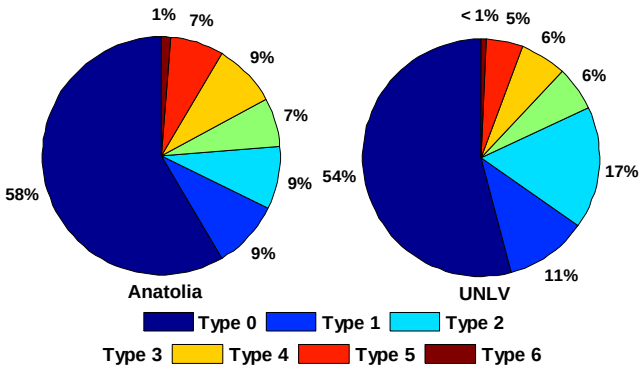

Fig. 5: Percent of each average cloud type at Anatolia and UNLV.

7. CLOUD CATEGORY MODELING AVERAGE GROUND IRRADIANCE

As was seen in Fig. 3, the type of cloud impacts the percentage of sunlight transmitted through the cloud. To analyze this, the average clear sky index is calculated for each daylight hour for the 60 minute period around each satellite image. Daylight hours are determined using the modeled clear sky irradiance and results in approximately 8500 hours during the time period. The clear sky index for each hour is plotted in Fig. 6 compared to the mean cloud type for Anatolia. Note that the order has been changed with type 5 (optically thin ice cloud) plotted between type 2 (water cloud) and type 3 (supercooled cloud) instead of with the optically thick clouds (type 4). A clear trend and average clear sky index can be associated with cloud type, although there is considerable scatter.

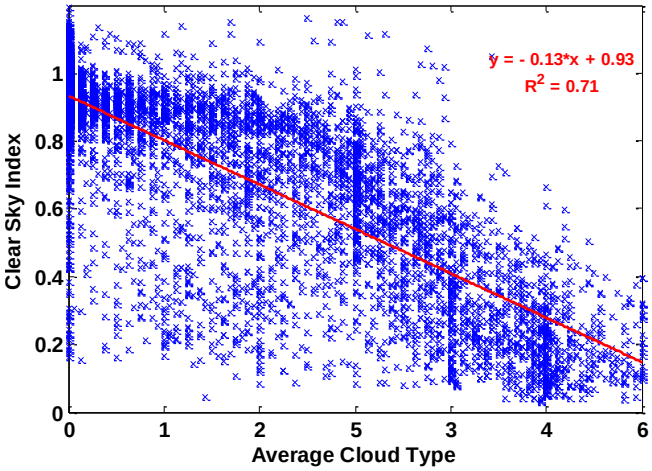

Fig. 6: Measured clearness index at Anatolia compared to GSIP cloud categories during all daylight hours.

The distribution of clear sky index for each cloud type is shown in Fig. 7. This is another way of visualizing how the average and spread of the measured clear sky index is dependent on the cloud category. In [22], the frequency distribution of clear sky index is listed at the first criteria for characterizing irradiance time series, and the second criteria considering ramp rates is discussed later. The mean clear sky index for the cloud type is shown with a vertical red line, and both the numeric values for the mean and mode clear sky index are noted on the plots. To verify the results are consistent for different locations, the same figure is presented for UNLV in Fig. 8, showing very similar distribution shapes and averages for clear sky index by cloud type.

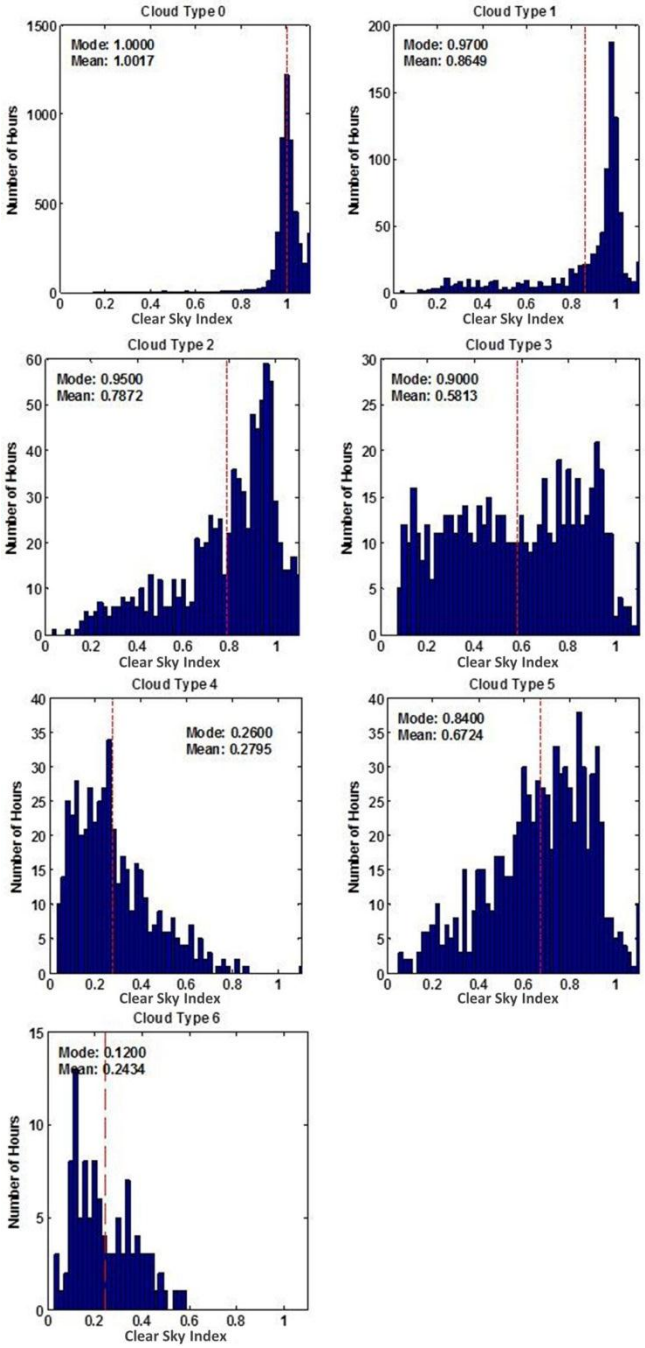

Fig. 7: Measured clear sky index at Anatolia compared to GSIP cloud categories.

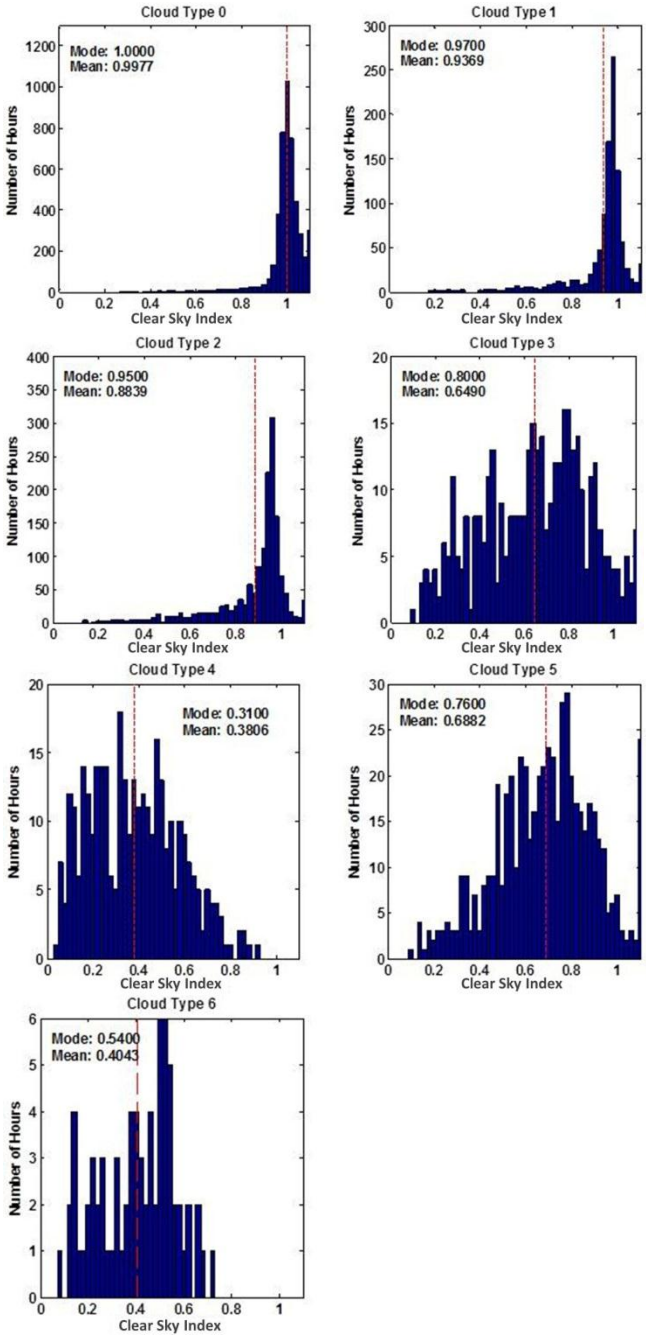

Fig. 8: Measured clear sky index at UNLV compared to GSIP cloud categories

8. CLOUD CATEGORY MODELING SOLAR VARIABILITY

The average clear sky index was shown to be dependent on the cloud type, and the variability is also influenced by the cloud category. Irradiance variability can be defined and calculated many different ways, but the easiest method is to calculate the standard deviation of the time series data. Similar to [4], the mean and standard deviation of clear sky index for the period 30 minutes on either side of the image are plotted in Fig. 9. This illustrates that types of clouds are generally in certain regions of the graph with specific clear sky indices and variability.

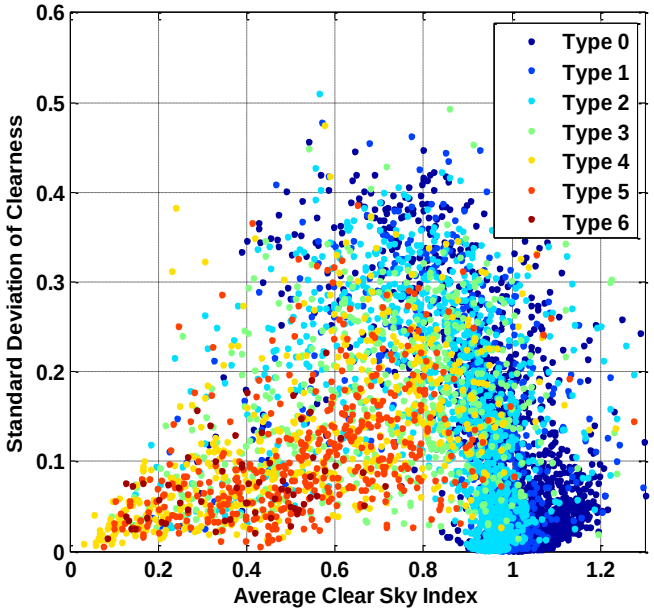

Fig. 9: Mean and standard deviation for the 1-hour clear sky index time series around the cloud type image for daylight hours at UNLV.

A metric for measuring variability called Variability Index (VI) was proposed in [23]. For the hour around the image, VI is calculated as:

$$VI = \frac{\sum_{k=2}^{n} \sqrt{(GHI_k - GHI_{k-1})^2 + \Delta t^2}}{\sum_{k=2}^{n} \sqrt{(CSI_k - CSI_{k-1})^2 + \Delta t^2}} \quad (1)$$

where *GHI* is a vector of length *n* of global horizontal irradiance values measured at some time interval in minutes, Δt, *CSI* is a vector of calculated clear sky horizontal irradiance for the same times as the *GHI* data. The average VI for each cloud type is shown in Fig. 10. Note that the shape of the variability by cloud type is very similar between the two locations. The plots in Fig. 10 show the daylight hours binned by the different statistics that can be calculated for the 16 cloud type pixels during each daylight hour. By using these statistics, some interesting insights can be drawn, such as that if there is Type 2 cloud without Type 0 or Type 1, VI is high. It can also be noted that Type 4 in generally has lower variability, like was noted in Fig. 3.

The same analysis as shown in Fig. 10 is performed for the standard deviation of the clear sky index for the hourly periods. The average of the hourly standard deviations binned by cloud type is shown in Fig. 11. Note the similarity between the patterns in Fig 10 and 11 for variability measured by VI or by standard deviation. Notice that the standard deviation increases with the range of cloud categories. It makes sense that cropped images with a larger difference between the maximum and minimum cloud type would have more variability in the irradiance profile during that period.

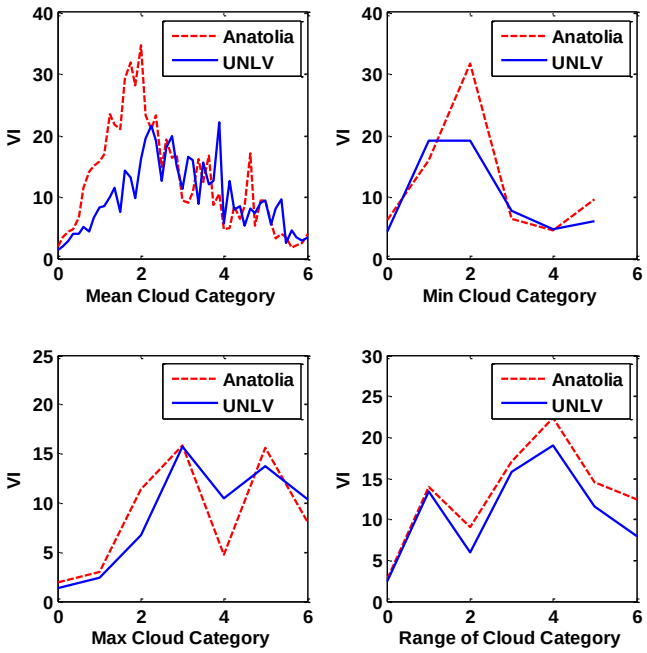

Fig. 10: Average VI by cloud type for each daylight hour at UNLV and Anatolia.

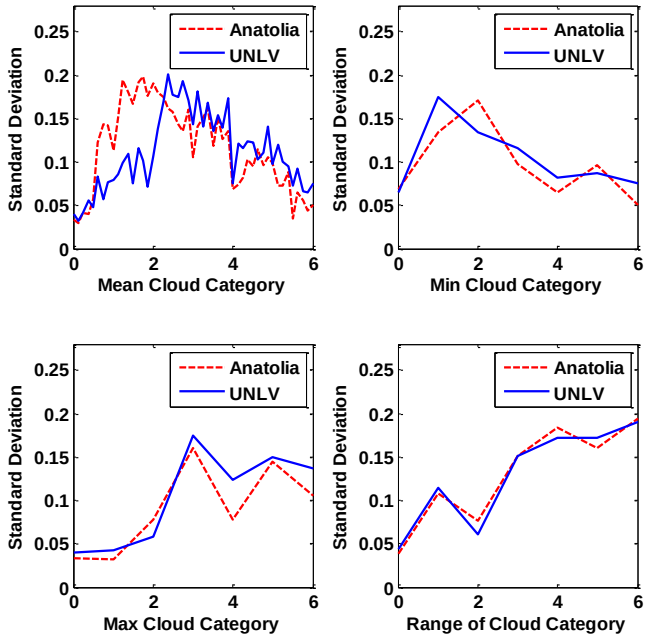

Fig. 11: Average of the 60-minute standard deviation of clear sky index for each daylight hour at UNLV and Anatolia compared to GSIP cloud category.

9. CLOUD CATEGORY MODELING RAMP RATES

Another method to characterize irradiance variability is to measure the magnitude of the ramp rates. The magnitude and frequency of the irradiance time series variability was previously discussed using VI and standard deviations, and the rate of the increase and decrease of irradiance is characterized using the ramp rate. Ramp rates are often compared between sites, different time scales, or between irradiance and power output, but our study compares ramp rates for different cloud categories. The 1-minute ramp rate is calculated as the absolute value of the difference between the clear sky index at each minute. The cumulative distribution function (CDF) for the 1-minute ramp rates during each cloud type are shown in Fig. 12 for Anatolia and UNVL from April 2009 to July 2011. The first graph is grouped by the mean cloud type in the 4x4 pixel satellite image, and the second row is grouped by the largest cloud number in the window. Even with the limited analysis dataset, it appears to be fairly consistent as to which clouds have higher ramp rates, independent of location. For example, a ramp rate of >0.4/minute for a mean cloud type of Type 2 (1.5% of the time at UNLV, and 3% of the time at Anatolia) is around 10 times more likely than if the mean cloud type is Type 0 or Type 5 (0.15% of the time at UNLV, and 0.3% of the time at Anatolia). Looking at the maximum cloud type, a ramp rate of >0.4/minute for a maximum cloud type of Type 3 (2% of the time) is 4 times more likely than if the maximum cloud type is Type 4 or Type 6 (0.5% of the time). If the ramp rates can be precisely correlated to cloud type, the expected distribution of ramp rates for a location can be determined by the distribution of cloud types in historical satellite imagery.

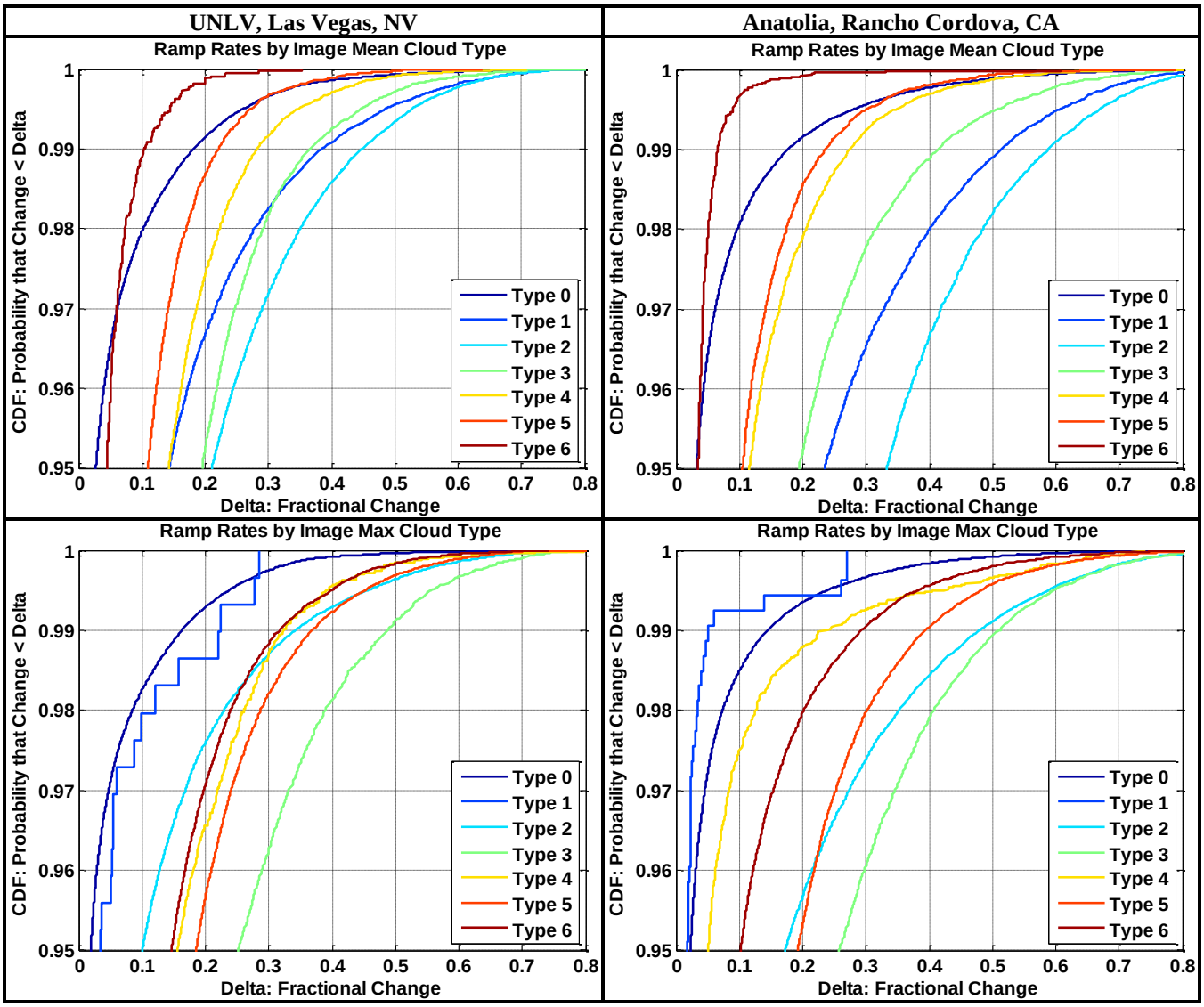

Fig. 12: CDF of the 1-minute ramp rates for two locations by cloud type.

10. CONCLUSION

The NOAA classification of cloud type is useful for characterizing the irradiance during the time period. Hourly cloud classified satellite images are compared to multiple years of ground measured irradiance at several locations to determine if measured irradiance, ramp rates, and variability index are correlated with cloud category. It was shown that the mean value and distribution of ground irradiance, the variability, and the distribution of ramp rates are dependent on the cloud category. Many studies have compared ramp rates between sites, time scales, and between irradiance and power output, but this paper presents a novel comparison of ramp rates and cloud categories, defined from satellite imagery. Using this method to model irradiance and variability from cloud type, satellite imagery and the prevalence of each cloud type at a location can be used to produce synthetic time series irradiance or represent the long-term irradiance distribution and variability profile for the location.

11. REFERENCES

[1] R. J. Broderick, J. E. Quiroz, M. J. Reno, A. Ellis, J. Smith, and R. Dugan, "Time Series Power Flow Analysis for Distribution Connected PV Generation," Sandia National Laboratories SAND2013-0537, 2013.

[2] M. J. Reno, A. Ellis, J. Quiroz, and S. Grijalva, "Modeling Distribution System Impacts of Solar Variability and Interconnection Location," in *World Renewable Energy Forum*, Denver, CO, 2012.

[3] R. Tapakis and A. G. Charalambides, "Equipment and methodologies for cloud detection and classification: A review," *Solar Energy*, 2013.

[4] C. E. Duchon and M. S. O'Malley, "Estimating cloud type from pyranometer observations," *Journal of Applied Meteorology*, vol. 38, p. 132, 1999.

[5] A. Orsini, C. Tomasi, F. Calzolari, M. Nardino, A. Cacciari, and T. Georgiadis, "Cloud cover classification through simultaneous ground-based measurements of solar and infrared radiation," *Atmospheric Research*, vol. 61, pp. 251-275, 2002.

[6] J. Calbó, J.-A. González, and D. Pagès, "A Method for Sky-Condition Classification from Ground-Based Solar Radiation Measurements," *Journal of Applied Meteorology*, vol. 40, p. 2193, 2001.

[7] T. P. DeFelice and B. K. Wylie, "Sky type discrimination using a ground-based sun photometer," *Atmospheric Research*, vol. 59-60, pp. 313-329, 2001.

[8] M. Martínez-Chico, F. J. Batlles, and J. L. Bosch, "Cloud classification in a mediterranean location using radiation data and sky images," *Energy*, vol. 36, pp. 4055-4062, 2011.

[9] H. G. Beyer, A. Hammer, J. Luther, J. Poplawska, K. Stolzenburg, and P. Wieting, "Analysis and synthesis of cloud pattern for radiation field studies," *Solar Energy*, vol. 52, pp. 379-390, 1994.

[10] A. Kazantzidis, P. Tzoumanikas, A. F. Bais, S. Fotopoulos, and G. Economou, "Cloud detection and classification with the use of whole-sky ground-based images," *Atmospheric Research*, vol. 113, 2012.

[11] A. Heinle, A. Macke, and A. Srivastav, "Automatic cloud classification of whole sky images," *Atmospheric Measurement Techniques*, vol. 3, pp. 557-567, 2010.

[12] M. Hummon, E. Ibanez, G. Brinkman, and D. Lew, "Sub-Hour Solar Data for Power System Modeling from Static Spatial Variability Analysis," in *2nd International Workshop on Integration of Solar Power in Power Systems*, Lisbon, Portugal, 2012.

[13] NOAA. *NOAA's Comprehensive Large Array-data Stewardship System*. Available: http://www.class.ngdc.noaa.gov/saa/products/search?datatype_family=GSIP

[14] M. J. Reno, C. W. Hansen, and J. S. Stein, "Global Horizontal Irradiance Clear Sky Models: Implementation and Analysis," Sandia National Laboratories SAND2012-2389, 2012.

[15] C. A. Gueymard, "Clear-sky irradiance predictions for solar resource mapping and large-scale applications: Improved validation methodology and detailed performance analysis of 18 broadband radiative models," *Solar Energy*, vol. 86, pp. 2145-2169, 2012.

[16] P. Ineichen and R. Perez, "A new airmass independent formulation for the Linke turbidity coefficient," *Solar Energy*, vol. 73, pp. 151-157, 2002.

[17] F. Kasten and A. T. Young, "Revised Optical Air-Mass Tables and Approximation Formula," *Applied Optics*, vol. 28, pp. 4735-4738, Nov 15 1989.

[18] W. L. Remund J., Lefevre M., Ranchin T., Page J., "Worldwide Linke turbidity information," in *Proceedings of ISES Solar World Congress*, Göteborg, Sweden, 2003.

[19] HelioClim. (2011, Feb.). *HelioClim Solar Radiation*. Available: http://www.helioclim.org/linke/linke_helioserve.html

[20] SoDa. (2011, Feb.). *Solar Radiation Data Service*. Available: http://www.soda-is.com/eng/index.html

[21] NREL. *Measurement and Instrumentation Data Center (MIDC)*. Available: http://www.nrel.gov/midc/

[22] C. W. Hansen, J. S. Stein, and A. Ellis, "Statistical Criteria for Characterizing Irradiance Time Series," Sandia National Laboratories SAND2010-7314, 2010.

[23] J. S. Stein, C. W. Hansen, and M. J. Reno, "The Variability Index: A New and Novel Metric for Quantifying Irradiance and PV Output Variability," in *World Renewable Energy Forum*, Denver, CO, 2012.

Sandia National Laboratories is a multi-program laboratory managed and operated by Sandia Corporation, a wholly owned subsidiary of Lockheed Martin Corporation, for the U.S. Department of Energy's National Nuclear Security Administration under contract DE-AC04-94AL85000.